Methodologies for Wind Turbine and STATCOM Integration in Wind Power Plant Models for Harmonic Resonances Assessment

Freijedo Fernandez, Francisco Daniel; Chaudhary, Sanjay K.; Guerrero, Josep M.; Teodorescu, Remus; Bak, Claus Leth

Published in:
Proceedings of the 14th Wind Integration Workshop

Publication date:
2015

Document Version
Early version, also known as pre-print

Methodologies for Wind Turbine and STATCOM Integration in Wind Power Plant Models for Harmonic Resonances Assessment

F. D. Freijedo, S. K. Chaudhary, J. M. Guerrero, R. Teodorescu and C. L. Bak
Department of Energy Technology, University of Aalborg,
Pontoppidanstraede 101, Aalborg 9220, Denmark.
{fran,skc,ret,joz,clb}@et.aau.dk

***Abstract*—This paper approaches modelling methodologies for integration of wind turbines and STATCOM in harmonic resonance studies. Firstly, an admittance equivalent model representing the harmonic signature of grid connected voltage source converters is provided. A simplified type IV wind turbine modelling is then straightforward. This linear modelling is suitable to represent the wind turbine in the range of frequencies at which harmonic interactions are likely. Even the admittance method is suitable both for frequency and time domain studies, some limitations arise in practice when implementing it in the time-domain. As an alternative, a power based averaged modelling is also proposed. Type IV wind turbine harmonic signature and STATCOM active harmonic mitigation are considered for the simulation case studies. Simulation results provide a good insight of the features and limitations of the proposed methodologies.**

I. Introduction

Wind power plants (WPPs) are usually located in remote areas, where bigger wind resources are available. In remote areas, the short-circuit power tends to be small, so the term "weak grid" is usually associated to WPP. In this scenario, voltage regulation and power quality and stability phenomena become a challenge [1].

Electric resonance is one of the most challenging scenario for WPP operation. Resonance issues arise in WPPs because their circuits contain both inductive and capacitive elements, which interact with active components [2]. From the wind energy industry perspective, this poses a collection of practical problems which can be summarized as follows [3]:

- A certain harmonic voltage or current level may be unacceptable because it results in damage to equipment, mal-operation of equipment, loss-of-life-of-equipment or other practical concerns. E.g., resonances can cause stability problems in the closed-loop controllers of grid-connected converters.
- A second type of unacceptability occurs when the limits set in the main applicable standards, such as EN-50160, IEC $61000-2-2$ and IEC $61000-3-6$. Furthermore, the limits set by the transmission system operators (TSOs) in the grid codes should be considered.

Therefore, WPP circuit analysis and modelling are an important topic of research in order to assess potential resonance issues and also to address the effectiveness of passive/active mitigation techniques.

This work proposes different modelling approaches able to represent Type IV wind turbine (WT) and STATCOM devices in the range of frequencies at which harmonic interactions are likely. The models are suitable for different kind of software tools, such as Matlab/Simulink, PSCAD, digSilent PF, etc.

Firstly, an admittance based approach for voltage source converter (VSC) is provided [4], [5]. The main assumptions made to look for a linear model is based on the previous experience in traction applications: the EN-50388 standard recommends to address harmonic instability issues as a linear phenomenon [6]. The proposed modelling represents the harmonic interactions between the active device and the rest of the grid, i.e., the VSC harmonic signature. As shown below, the admittance explicitly includes the main VSC control and hardware parameters.

In practice, it has been found that the admittance model is more suitable for frequency domain analysis. In time domain simulation the admittance has to be implemented with the combination of a current source and a discretized transfer functions, which poses some practical limitations that are discussed below.

As an alternative, a power based averaged model is then proposed aiming for a low computational burden time domain simulations [7], [8]. This model strategy explicitly includes the VSC control loops, but substitutes the switching devices by ideal current and voltage sources driven by the averaged VSC voltage/power equations. The averaged method has been also found effective to represent the dynamics of active components in harmonic resonance scenarios.

Two different study cases are analyzed with simulation results. Firstly, a simplified type IV WT admittance is derived. Its equivalence with the averaged based method is then proved from the time-domain steady-state current spectrum [6]. This result supports the suitability of using admittance models in frequency domain analyses related to harmonics resonances in WPP. In this context, some features of the WT admittance are discussed. Subsequently, an averaged STATCOM model with active damping functionality [9] is tested in a complex WPP model. It is shown how the STATCOM successfully performs in steady and transient states. Operation waveforms are obtained for both ac and dc sides of the STATCOM.

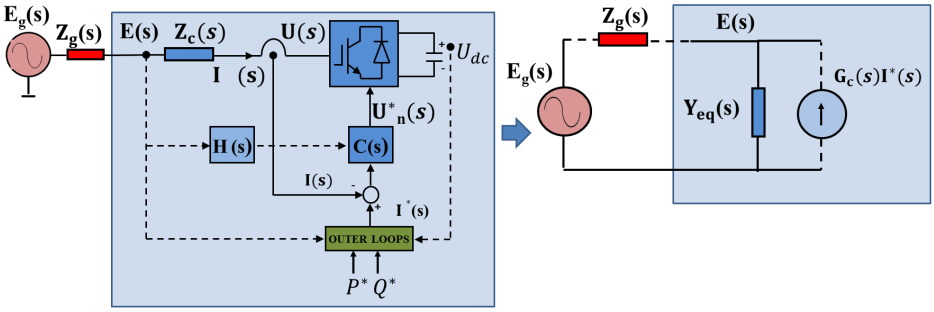

Fig. 1. Modelling of a grid-connected power electronics converter by its equivalent admittance $\mathbf{Y}_{\text{eq}}(s)$.

II. Admittance Based Modelling of Grid-Connected Power Converters

This section details how to obtain a simplified admittance model for grid-connected VSC working in a linear region. It aims to represent the VSC dynamics interaction when connected at any point of the power system.

1) Derivation of the Model: The output current of the converter in Fig. 1 is given by

$$\mathbf{I}(s) = \mathbf{G}_{\text{c}}(s)\mathbf{I}^*(s) + \mathbf{Y}_{\text{eq}}(s)\mathbf{E}(s) \tag{1}$$

with $\mathbf{G}_{\text{c}}(s)$ being the closed loop transfer function and $\mathbf{Y}_{\text{eq}}(s)$ an equivalent Norton admittance. These two parameters are obtained as follows. The grid current $\mathbf{I}(s)$ is

$$\mathbf{I}(s) = \mathbf{Z}_{\text{c}}^{-1}(s)[\mathbf{E}(s) - \mathbf{U}(s)] \tag{2}$$

with $\mathbf{Z}_{\text{c}}(s)$ being the converter output filter impedance and $\mathbf{U}(s)$ the output voltage. On the other hand, the converter control law $\mathbf{U}^*(s)$ (PWM reference) is defined by

$$\mathbf{U}^*(s) = -\mathbf{C}(s)[\mathbf{I}^*(s) - \mathbf{I}(s)] + \mathbf{U}(s)\mathbf{H}(s) \tag{3}$$

with $\mathbf{C}(s)$ the controller and $\mathbf{H}(s)$ the voltage feed-forward transfer functions, respectively. If system delays (due to discrete-time operation) are neglected, $\mathbf{U}(s) = \mathbf{U}^*(s)$ is assumed. This leads to the following expressions

$$\begin{aligned} \mathbf{G}_{\text{c}}(s) &= \frac{\mathbf{C}(s)}{\mathbf{Z}_{\text{c}}(s) + \mathbf{C}(s)} \\ \mathbf{Y}_{\text{eq}}(s) &= \frac{1 - \mathbf{H}(s)}{\mathbf{Z}_{\text{c}}(s) + \mathbf{C}(s)} \end{aligned} \tag{4}$$

for the closed loop controller and admittance in (1).

2) Control Bandwidth Considerations: The previous approach has been derived by assuming that there is not effect of the system delays. If considered

$$\mathbf{U}(s) = \mathbf{U}^*(s)e^{-sT_d} = \mathbf{U}^*(s)e^{-s1.5/f_s} \text{ (ZOH + PWM effects)} \tag{5}$$

with T_d and f_s being the system delay and sampling frequency, respectively [5], [10], [11]. In order to avoid the positive feedback (instability), the bandwidth of $\mathbf{G}_{\text{c}}(s)$ is limited to $0.1f_s$ [11]. At the same time, f_s is limited by the PWM carrier frequency f_{pwm}. In a two-level VSC using a regular sampling PWM $f_s = f_{pwm}$ (single update) or $f_s = 2f_{pwm}$ (double update) [11]. Clearly, the former is preferred from the control perspective. An even more convenient relation between f_s and f_{pwm} can be achieved with multilevel converters [12]. On the other hand, commercial devices tend to reduce switching rates to control power losses [12], [13], so there is a clear tradeoff between control ability and power losses. Focusing on the modelling, it is clear that a good knowledge of the device is needed to accurately asses its achievable control bandwidth.

III. Average Model Based on AC-DC Power Balancing

A detailed model of the power converter, including non-linear effects, can be represented by software tools. Such a detailed operation is specially suitable to accurately represent many non-linear behavior of the power converter, such as PWM patterns [14]. However, this is at the cost of a high computational burden. Focusing on harmonic resonances in the WPP circuits, the inclusion of such detailed converter models is not always feasible, and then simplified models are usually required [1], [15].

The main assumption taken to simplify the VSC modelling is to consider its currents and voltages averaged over a switching cycle [7]. This assumption is available as the VSC switching frequency is higher than the range of potential resonance interactions with the WPP [15]. It can be expressed as follows:

$$\mathbf{U}(t) = 0.5[m_a(t)U_{dc}(t), m_b(t)U_{dc}(t), m_c(t)U_{dc}(t)] \tag{6}$$

with $U_{dc}(t)$ being the dc-link voltage and $[m_a(t), m_b(t), m_c(t)]$ being the control reference signals. Assuming an Space Vector Modulation (SVM-PWM) or equivalent for smart use of dc-link, the range of linear operation for the control signals is $[-1.15, 1.15]$ [14]. Since the VSC is a three-wire system, the output voltage can be set by two controlled voltage sources driven by two of the line to line voltages (the other one is linear dependent, and hence not explicitly needed).

Another assumption, which permits to consider the VSC dc-link dynamics, is to consider an ideal power conversion between ac and dc sides of the VSC [8]. Then, the dc-link current can be derived as follows

$$I_{dc}(t) = 0.5[m_a(t)I_a(t) + m_b(t)I_b(t) + m_c(t)I_c(t)] \tag{7}$$

with $I_a(t), I_b(t), I_c(t)$ being the ac-currents. Then, the dc-current is implemented by a controlled current source.

Fig. 2 shows the implementation of the average model. "Memory blocks" (i.e., a one-simulation-step delay) should be introduced between measured signals and source commands to avoid algebraic loops.

This methodologies explicitly considers converter control blocks in the time-domain. Then, advanced controllers such

as the ones used for short-term stability (e.g. low voltage ride through requirements for WTs) can be included in the controller. Therefore, averaged modelling can be also considered to assess many of the functionalities explicit in IEC-61400-27, IEC-61400-21-1 and IEC-61400-21-2 [16]. Anyway, it should be bore in mind that for harmonic studies, simulation time steps should be reduced (at the cost of computational burden) to increase the frequency resolution.

IV. Case Studies and Simulation Results

Two different case studies are provided to show the features and performance of the proposed VSC modelling techniques. Simulation results have been obtained with PLECS.

A. Admittance Model Verification for a Type IV WT

Table I shows the parameters employed for modelling the grid VSC of a Type IV WT. The VSC is connected to the grid through an LCL converter [17], [18]. In order to simplify the analysis, SISO expressions are used (cross-coupling effects are neglected) [10]. Then, $\mathbf{C}(s)$ is now considered a SISO proportional controller $C(s)$ obtained by internal model control [5]. It should be noted that, for a LCL filter connection, $Y_{eq}(s)$ only represents the VSC dynamics set by $C(s)$ and the converter filter $Z_c(s)$ [5]. $Z_{c2}(s)$ and $Z_{tf}(s)$ remain as passive components of the circuit.

TABLE I
Type IV Wind turbine model and Test

Parameter	Value
Grid parameters (test)	
Fundamental angular frequency	$\omega_1 = 2\pi 50\,\mathrm{rad/s}$
Voltage	$690\,\mathrm{V_{rms}}$
LCL filter	
Converter filter Inductance	$Z_c = 0.01 + 0.1\,\mathrm{p.u.}$ (resistive+inductive)
Capacitor	$Z_{c2} = 0.05\,\mathrm{p.u.}$ (capacitive)
Transformer leakage	$Z_{tf} = 0.1\,\mathrm{p.u.}$ (inductive)
LCL resonance frequency	$1\,\mathrm{kHz}$ (from Z_c, Z_{c2}, Z_{tf})
Ideal Controller	
Current controller bandwidth	$\alpha_{cc} = 250\,\mathrm{Hz}$
Feedforward LPF cut-off	$\alpha_{LPF} = 400\,\mathrm{Hz}$

Fig. 3 shows the simulation model used to validate the equivalence between admittance and averaged modelling. The admittance is implemented in the time domain by means of a controlled current source driven by $E(t) * Y_{eq}(t)$. In order to avoid algebraic loops, $Y(s)$ should be discretized, so $Y(t)$ remains strictly proper [19].

Fig. 4 shows the steady-state harmonic spectrum obtained from the tests in Fig. 3. It can be checked the equivalence between both models.

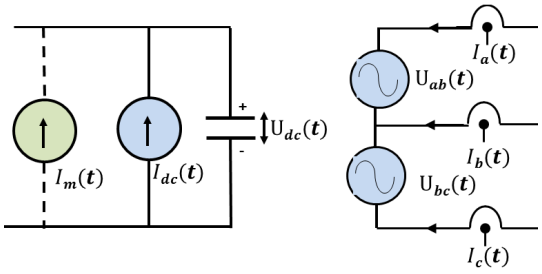

Fig. 2. Average VSC block diagram.

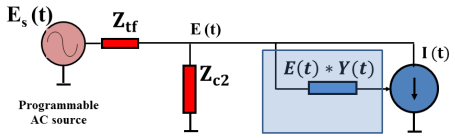

(a) Admittance implementation.

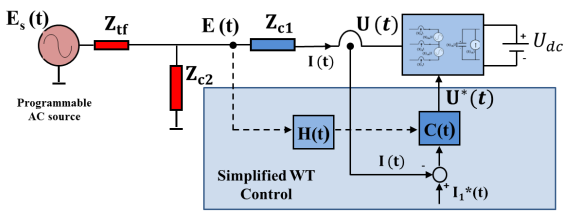

(b) Average converter implementation.

Fig. 3. Tests to measure the WT harmonic signature according to EN-50388: the voltage harmonics are programmed in $\mathbf{E}(s)_g$ and then the current harmonics are measured at the VSC point of connection.

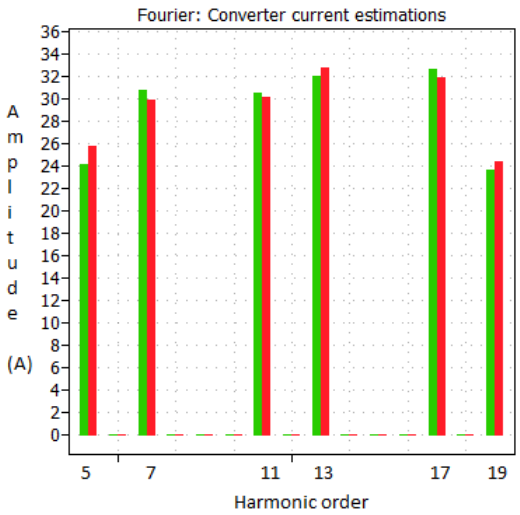

Fig. 4. Fourier components obtained in time-domain from admittance (green) and averaged (red) models.

1) Physical Interpreation of $Y_{eq}(s)$ (Frequency Domain): Fig. 5 shows the frequency domain representation for the admittance obtained [from Table I and (4)]. It can be observed that the admittance, is well damped at low frequencies, where the proportional part of the control is dominant over $Z_{c1}(s)$. At higher frequencies, the control action is not effective and $Y_{eq}(s)$ mainly represents the inductive filter represented by $Z_{c1}(s)$. The admittance tends to be more and more undamped as its phase-angle tends to $-90\,\mathrm{deg}$. If system delays (due to discrete time control operation) are included for a more accurate analysis, the phase delay can be even below $-90\,\mathrm{deg}$, which describes a non-passive system [5]. If grid impedance [as seen from $E(s)$] is available, analyses based on the Nyquist stability criterion are suitable [5], [20]. E.g., if the wind turbine point of connection presents a high capacitive behavior at a frequency at which $Y_{eq}(s)$ is inductive, the sensitivity peak (minimum distance of the Nyquist trajectory to -1 [21]) tends to be small at such frequency. In fact, non passive system may go to instability as a "negative resistance" represents a positive feedback in the control system. This kind of situations reflects potential harmonic resonance between the WT and the WPP.

On the other hand, it should be noted that the LCL filter presents a resonance which is set in the VSC design. If a reasonable sampling frequency is considered, this LCL resonance is around or even above 1 kHz [17], [18]. Therefore, in principle, a damp harmonic signature below LCL resonance frequencies is expected for Type IV WT.

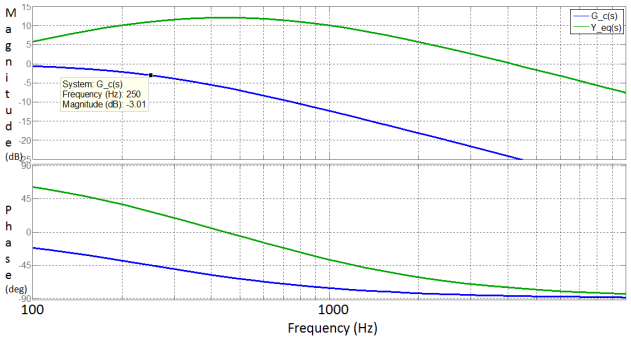

Fig. 5. Frequency domain representation of $G_c(s)$ and $Y_{eq}(s)$.

2) Features and Limitations of Admittance Modelling: As shown, the admittance modelling is specially suitable to represent the wind turbine harmonic signature in the frequency domain. A good insight of the wind turbine behavior can be obtained with a low order transfer function. However, for time domain simulations [see Fig. 3(a)], practical limitations have been found. Firstly, it has been checked that the sampling time should be quite reduced, which means an increase of the computational burden. This behavior can be expected from the inaccuracies introduced at $Y_{eq}(s)$ discretization (a process needed for discrete-time operation, usually software tools implement it automatically) which introduces extra phase at high frequencies [19]. From the Nyquist stability criterion, this extra phase tends to make the system unstable, so the sampling time reduction is needed to enhance the accuracy. Clearly, this is at the cost of increase the computational burden. Furthermore, if a good representation of the fundamental component behavior is wanted, more blocks are needed [$G_c(s)$, resonant/integral control action in $C(s)$, outer loops [4], etc.], which increases the order and complexity of the model too much.

B. Averaged Model of STATCOM with Active Filtering

The aim of this section is to show the average based modelling implementing active filtering for harmonic resonance mitigation [22]. Fig. 6 depicts a single-line representation of a STATCOM with active filtering included in a detailed WPP model, also implemented in PLECS. The WPP circuit presents potential harmonic voltage amplifications at some points due to resonances with the external grid impedance.

Fig. 7 shows the effect of a resonance between the external source and T2: a voltage harmonic amplification at the 5^{th} harmonic component (1.58 multiplication factor) is likely.

Table II represents the STATCOM parameters and values employed in the simulation. Active filtering operation is based on a state feedback of the voltage at the point of connection [23], [24]. The 5^{th} harmonic is obtained in real time by Discrete Fourier Transform (DFT) [25].

Fig. 8 shows simulated waveforms for the voltage at the point of STATCOM connection [$E_{pcc}(t)$] and STATCOM current [$I_c(t)$]. Fig. 8(a) shows the waveforms in the whole

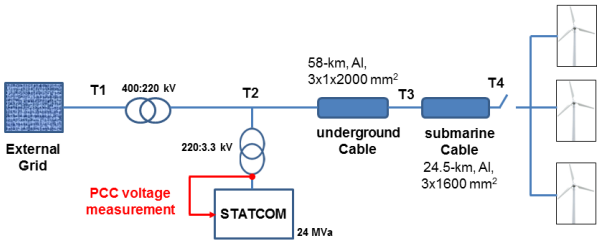

(a) Single-line diagram of WPP circuit and STATCOM.

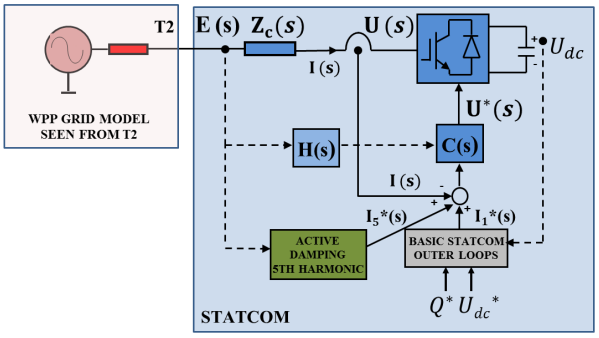

(b) STATCOM controller representation.

Fig. 6. Simplified problem formulation: the STATCOM at T2 includes active filtering functionality to mitigate harmonic amplifications at the PCC voltage due to a series resonance.

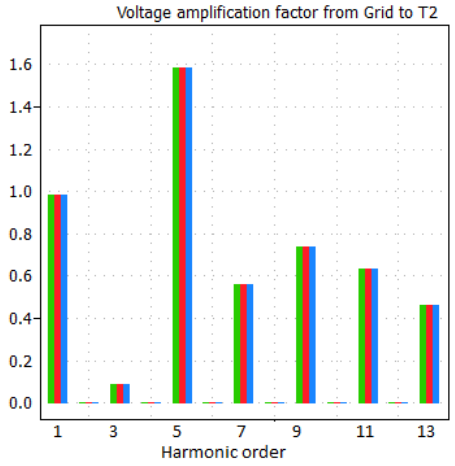

Fig. 7. Voltage amplification factor between the external grid and T2.

TABLE II
STATCOM MODEL PARAMETERS

Parameter	Value
External Grid	
Fundamental angular frequency	$\omega_1 = 2\pi 50\,\mathrm{rad/s}$
Programmed 5^{th} background harmonics	0.0100 p.u.
STATCOM Hardware	
Voltage level at STATCOM pcc	$3.3\,\mathrm{kV_{rms}}$
Output filter Inductance	$L_c = 40\,\mathrm{uH}$ and $R_c = 50\,\mathrm{m\Omega}$
Rated dc-link voltage	$U_{dc} = 5250\,\mathrm{V}$
Dc-link capacitance	$C_{dc} = 40\,\mathrm{mF}$
Fundamental angular frequency	$\omega = 2\pi 50\,\mathrm{rad/s}$
STATCOM Control	
Dc-link voltage controller bandwidth	$\alpha_{dc} = 7\,\mathrm{Hz}$
Main Current controller bandwidth (fundamental component controller)	$\alpha_{cc} = 100\,\mathrm{Hz}$
Active damping gain (effective at the 5^{th} harmonic)	$K_{ad}^{'} = -3$

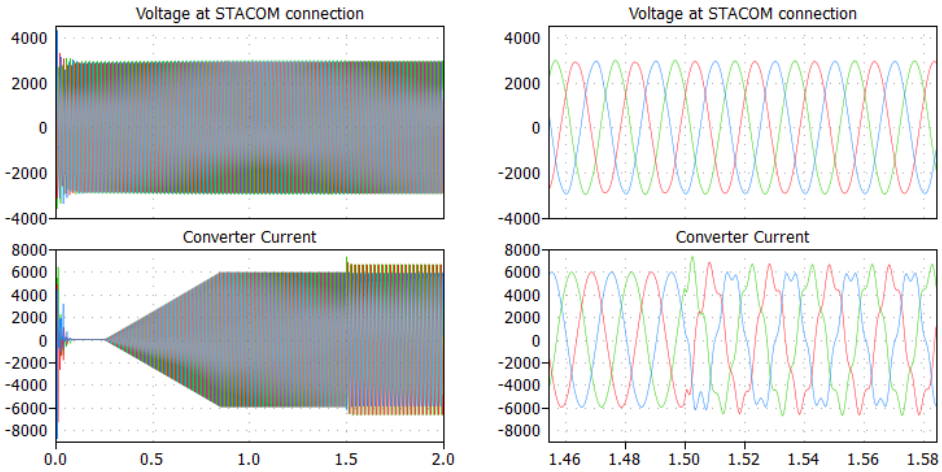

(a) E_{pcc} and I_c along the simulation.

(b) E_{pcc} and I_c detailed at the moment of active filtering activation.

Fig. 8. E_{pcc} and I_c waveforms.

simulation time window of 2 seconds. It can be appreciated how, after an initial transient, the reactive current reference starts to increase in ramp up to $Q = 24\,\text{MVA}$ (the main STATCOM functionality). Then, the rated reactive current is reached. Subsequently, at 1.5 seconds the active filtering functionality is enabled. It can be appreciated how the current waveforms changes. Fig. 8(b) shows the detail of Fig. 8(a) at the moment of the activation of active filtering functionality: when active damping is activated, the 5^{th} harmonic current jumps increases from 0 to 0.13 p.u (the improvement in the voltage waveform is not clear by time domain inspection, so frequency spectrum analysis, as shown below in Table III, is needed). This suggests that a highly distorted current at the output of the STATCOM is demanded to perform active filtering.

Fig. 9 shows the 5^{th} harmonic at the STATCOM connection $[E_{pcc5}(t)]$ when active damping is enabled. It can be seen how the 5^{th} harmonic is attenuated by around a half.

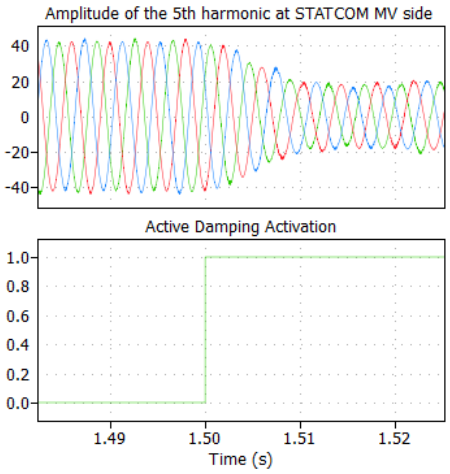

Fig. 9. $E_{pcc5}(t)$ at STATCOM PCC when the active filtering option is enabled.

Table III represents the steady-state values for the 5^{th} harmonic voltage at different points of the WPP (see Fig. 6), both when the active filtering is disabled or enabled.

TABLE III
VOLTAGE AMPLITUDE OF THE 5^{th} HARMONIC COMPONENT

Active Filtering Disabled				
Background	T1	T2	T3	T4
0.0100 p.u.	0.0147 p.u.	0.0158 p.u.	0.0086 p.u.	0.0140 p.u.
Active Filtering Enabled				
Background	T1	T2	T3	T4
0.0100 p.u.	0.0099 p.u.	0.0076 p.u.	0.0045 p.u.	0.0074 p.u.

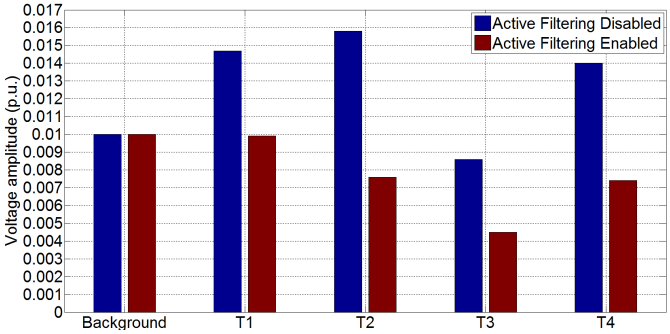

Fig. 10 shows how the dc-link controller effectively regulates the dc-bus voltage (i.e., steady-state zero error is achieved and transitory disturbances rejected). It can be also appreciated the transient effects of reactive current changes and active filtering enabling: during the change in the reactive current reference, there is a drop in the dc-link voltage (disturbance effect), which is compensated when the reference reaches the final value; when the active filtering is enabled, a dc-link ripple corresponding with the resonance frequency in the synchronous reference frame arises (in this simulation, the 5^{th} order harmonic is converted into a 6^{th} order harmonic ripple in the dc-link). A high capacitance value seems recommended to minimize these effects.

Fig. 10 also shows the control signals. It has been checked that the STATCOM is working in linear zone, as the saturation limits at $[-1.15, 1.15]$ are not reached in steady-state. The dc-link capacitance value and a dc-link voltage reference have a decisive impact to keep the STATCOM working in linear zone. Ideally, both parameters should be high, but this

would be at the cost of size and cost of the capacitance and switching technology (e.g., maximum DC-link voltage is a key factor in IGBT selection).

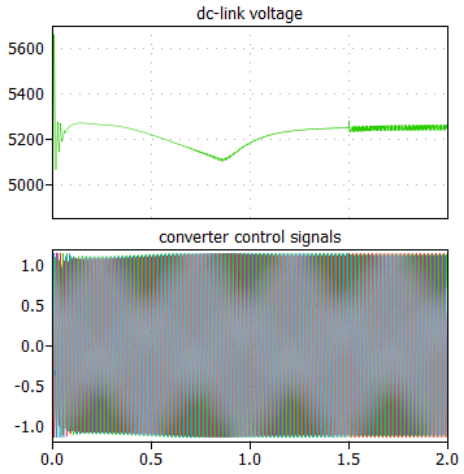

Fig. 10. Dc-link voltage and control references $[m_a(t), m_b(t), m_c(t)]$.

V. Conclusion

This paper provides different methodologies for modelling wind turbines and STATCOM in large WPP harmonic resonance studies. An admittance based model is derived, which includes the effect of control and hardware filters. It is proved that this modelling strategy is specially suitable for frequency domain studies. It can be observed that the effect of control is to damp the response at low frequencies (below the current control bandwidth). The admittance expression is suitable to represent advanced control techniques (e.g., a voltage feedforward path) and sampling delays. A good knowledge of wind turbine VSC parameters, such as LCL filter or sampling frequency will help to provide accurate modelling. For studies in the time-domain, an average power based VSC model has been found as a more efficient alternative. As an example of its features, a STATCOM case study is provided. Simulation results shows the active filtering functionality in the WPP circuit (ac-side), but also represents the dynamics in the VSC dc-side (i.e., dc-link capacitance and outer voltage dynamics, and amplitude modulation index).

Acknowledgment

This work is supported by Energinet.dk through the project "Active filter functionalities for power converters in Wind Power Plants" [Forskel program, project number 2014-1-12188 (PSO)].

References

[1] N. Strachan and D. Jovcic, "Stability of a variable-speed permanent magnet wind generator with weak AC grids," *IEEE Trans. Power Del.*, vol. 25, no. 4, pp. 2779–2788, 2010.

[2] M. Bradt, B. Badrzadeh, E. Camm, D. Mueller, J. Schoene, T. Siebert, T. Smith, M. Starke, and R. Walling, "Harmonics and resonance issues in wind power plants," in *IEEE Power and Energy Society General Meeting*, San Diego, CA, 2011, pp. 1–8.

[3] R. Zheng and M. Bollen, "Harmonic resonances associated with wind farms," Lulea Univ. of Technology, Skelleftea, Tech. Rep., Jul. 2010.

[4] L. Harnefors, M. Bongiorno, and S. Lundberg, "Input-admittance calculation and shaping for controlled voltage-source converters," *IEEE Trans. Ind. Electron.*, vol. 54, no. 6, pp. 3323–3334, 2007.

[5] L. Harnefors, A. Yepes, A. Vidal, and J. Doval-Gandoy, "Passivity-based controller design of grid-connected vscs for prevention of electrical resonance instability," *IEEE Trans. Ind. Electron.*, vol. 62, no. 2, pp. 702–710, 2015.

[6] *EN50388. Railway Applications – Power supply and rolling stock – Technical criteria for the coordination between power supply (substation) and rolling stock to achieve interoperability*, Cenelec Std., 2012.

[7] D. Maksimovic, A. Stankovic, V. Thottuvelil, and G. C. Verghese, "Modeling and simulation of power electronic converters," *Proc. IEEE*, vol. 89, no. 6, pp. 898–912, 2001.

[8] V. Blasko and V. Kaura, "A new mathematical model and control of a three-phase AC-DC voltage source converter," *IEEE Trans. Power Electron.*, vol. 12, no. 1, pp. 116–123, 1997.

[9] L. Kocewiak, J. Hjerrild, and C. Bak, "Wind turbine converter control interaction with complex wind farm systems," *IET Renewable Power Generation*, vol. 7, no. 4, pp. 380–389, 2013.

[10] F. Freijedo, A. Vidal, A. Yepes, J. Guerrero, O. Lopez, J. Malvar, and J. Doval-Gandoy, "Tuning of synchronous-frame pi current controllers in grid-connected converters operating at a low sampling rate by MIMO root locus," *IEEE Trans. Ind. Electron.*, vol. 62, no. 8, pp. 5006–5017, 2015.

[11] D. G. Holmes, T. A. Lipo, B. McGrath, and W. Kong, "Optimized design of stationary frame three phase AC current regulators," *IEEE Trans. Power Electron.*, vol. 24, no. 11, pp. 2417–2426, Nov. 2009.

[12] M. Odavic, V. Biagini, M. Sumner, P. Zanchetta, and M. Degano, "Low carrier–fundamental frequency ratio PWM for multilevel active shunt power filters for aerospace applications," *IEEE Trans. Ind. Appl.*, vol. 49, no. 1, pp. 159–167, 2013.

[13] O. Senturk, L. Helle, S. Munk-Nielsen, P. Rodriguez, and R. Teodorescu, "Power capability investigation based on electrothermal models of press-pack IGBT three-level npc and anpc vscs for multimegawatt wind turbines," *IEEE Trans. Power Electron.*, vol. 27, no. 7, pp. 3195–3206, 2012.

[14] G. Holmes and T. Lipo, *Pulse Width Modulation for Power Converters: Principles and Practices*. John Wiley & Sons, 2003.

[15] B. Badrzadeh, M. Gupta, N. Singh, A. Petersson, L. Max, and M. Hogdahl, "Power system harmonic analysis in wind power plants — Part I: Study methodology and techniques," in *Industry Applications Society Annual Meeting (IAS), 2012 IEEE*, 2012.

[16] P. Sorensen, J. Fortmann, F. J. Buendia, J. Bech, A. Morales, and C. Ivanov, "Final draft international standard iec 61400-27-1," in *Proc. of the 13th Wind Integration Workshop*, 2014.

[17] J. Dannehl, F. Fuchs, S. Hansen, and P. Thogersen, "Investigation of active damping approaches for pi-based current control of grid-connected pulse width modulation converters with LCl filters," *IEEE Trans. Ind. Appl.*, vol. 46, no. 4, pp. 1509–1517, 2010.

[18] G. Gohil, L. Bede, R. Teodorescu, T. Kerekes, and F. Blaabjerg, "Line filter design of parallel interleaved vscs for high power wind energy conversion system," *IEEE Trans. Power Electron.*, to be published, early Access.

[19] G. C. Goodwin, S. F. Graebe, and M. E. Salgado, *Control System Design*. Prentice Hall, 2000, ch. 12.

[20] J. Sun, "Impedance-based stability criterion for grid-connected inverters," *IEEE Trans. Power Electron.*, vol. 26, no. 11, pp. 3075–3078, 2011.

[21] A. Yepes, F. Freijedo, O. Lopez, and J. Doval-Gandoy, "Analysis and design of resonant current controllers for voltage-source converters by means of Nyquist diagrams and sensitivity function," *IEEE Trans. Ind. Electron.*, vol. 58, no. 11, pp. 5231–5250, 2011.

[22] L. Kocewiak, S. Chaudhary, and B. Hesselbaek, "Harmonic mitigation methods in large offshore wind power plants," in *Proc. of The 12th International Workshop on Large-Scale Integration of Wind Power into Power Systems as well as Transmission Networks for Offshore Wind Farms*, 2013.

[23] H. Akagi, "Active harmonic filters," *Proc. IEEE*, vol. 93, no. 12, pp. 2128–2141, 2005.

[24] B. Ronner, "Harmonic voltage control with a statcom," in *Proc. of the 13th European Conference on Power Electronics and Applications (EPE)*, 2009.

[25] F. Freijedo, J. Doval-Gandoy, O. Lopez, P. Fernandez-Comesana, and C. Martinez-Penalver, "A signal-processing adaptive algorithm for selective current harmonic cancellation in active power filters," *IEEE Trans. Ind. Electron.*, vol. 56, no. 8, pp. 2829–2840, 2009.